land

MDPI

Article

Evaluation of the Construction Suitability and Sediment Reduction Potential of Dry-Farming Wide Terraces on Sloping Farmland in the Loess Plateau

Ying Han, Wenjing Wang, Xinjia Chen, Jinxia Fu *, Ruizhe Du and Bo Li

College of Natural Resources and Environment, Northwest A&F University, Xianyang 712100, China; hanying20000125@nwafu.edu.cn (Y.H.); wanwj@nwafu.edu.cn (W.W.); ruizhedu@nwafu.edu.cn (R.D.); 2283746344@nwafu.edu.cn (B.L.)

* Correspondence: fujinxia405@nwsuaf.edu.cn

Abstract

Assessing the construction suitability and sediment reduction potential of dry-farming wide terraces is critical for improving soil and water conservation in semi-arid and semi-humid regions, yet these aspects are seldom evaluated within an integrated framework. Focusing on the Loess Plateau, this study delineates potential construction areas based on precipitation constraints, quantifies soil erosion using the Revised Universal Soil Loss Equation, and develops a multidimensional framework to jointly evaluate construction suitability and sediment reduction potential on sloping farmland. Results indicate that slope, transportation accessibility, and soil erosion intensity are the primary determinants of suitability. Highly suitable, suitable, and marginally suitable areas account for 7.5%, 7.2%, and 4.3% of the study area, respectively, with Shanxi, Shaanxi, and Gansu provinces—and particularly Yulin, Yan'an, and Qingyang—emerging as priority regions for implementation. Scenario analysis suggests that targeting (i) highly suitable and suitable areas or (ii) all suitable classes would reclaim approximately 59.89 $\times$ 10^3 km^2 and 77.19 $\times$ 10^3 km^2 of sloping farmland, respectively, leading to reductions in mean soil erosion modulus of 16.6% and 22%. These findings provide a quantitative basis for optimizing terrace deployment and advancing regionally targeted soil erosion mitigation strategies on the Loess Plateau.

Keywords: wide terrace construction; land suitability evaluation; soil erosion control; RUSLE model; loess plateau

Check for updates

Academic Editor: Gregorio García-Fernández

Received: 10 March 2026
Revised: 16 April 2026
Accepted: 21 April 2026
Published: 28 April 2026

Copyright: © 2026 by the authors. Licensee MDPI, Basel, Switzerland. This article is an open access article distributed under the terms and conditions of the Creative Commons Attribution (CC BY) license.

1. Introduction

Soil erosion is widely considered one of the most urgent global environmental issues, and it poses a significant threat to regional ecosystems, agricultural productivity and economic development [1]. The Loess Plateau, located in the semi-arid and semi-humid region, is one of the most serious areas of soil and water loss in China, with an alarming soil and water loss ratio of up to 71%. Sloping farmland is a major source of soil and water loss in the Loess Plateau. Although sloping farmland occupies only 18% of the area of the Loess Plateau, it contributes more than 30% of the total soil erosion in the region [2]. Especially in some hilly regions, 70–90% of cultivated land is sloping farmland, with 15–20% of these plots having slopes greater than 25° [3]. With the increase in cultivated land slopes and intensive human utilization, soil erosion on sloping farmland in the Loess Plateau has become increasingly severe [4].

Dry-farming terraces, as a key measure for soil and water conservation and ecological restoration in the Loess Plateau, have played a significant role in improving sloping farmland, controlling soil erosion, increasing crop yield, ensuring ecological safety and promoting regional economic development [5–7]. Through long-term experimental research, demonstration and promotion by scientists and technology workers, dry-farming terraces in the Loess Plateau have evolved from manual terraces and machine-built terraces to advanced mechanized wide terraces, and from small and narrow terraces to contiguous and large-scale horizontal terraces [8]. In this study, a dry-farming wide terrace refers to a high-standard horizontal terrace constructed on sloping farmland, generally with a width greater than 10 m, which is suitable for mechanized farming operations and contiguous large-scale cultivation. Compared with traditional narrow terraces, wide terraces have a wider cultivation surface, more regular field configuration, greater soil and water conservation capacity, better crop production conditions, and more efficient utilization of soil and water resources. Furthermore, wide terraces are conducive to realizing large-scale farming, optimizing land use structure, and promoting ecological protection and economic development of the Loess Plateau [9]. However, at present, the following prominent problems still exist in the construction of dry-farming terraces in the Loess Plateau: a high proportion of manual narrow terraces (with widths less than 5 m), low construction standards, difficulties in mechanized farming operations, and an inability to meet the demands of agricultural modernization. Additionally, narrow terraces with low construction standards often become a major source of soil erosion under extreme weather conditions [8,9]. Consequently, the construction of high-standard dry-farming wide terraces (with widths greater than 10 m) will be a key measure for regulating sloping farmland and narrow terraces in the Loess Plateau. Thus, which areas are suitable for the construction of dry-farming wide terraces in the Loess Plateau? What are the suitability grades and constraints in these areas, and what is the sediment reduction potential after the construction of dry-farming wide terraces? To address these challenges, it is crucial to evaluate the construction suitability and sediment reduction potential of dry-farming wide terraces in the Loess Plateau. However, studies on the integrated evaluation of the construction suitability and sediment reduction potential of dry-farming wide terraces remain limited.

Currently, research on the suitability evaluation of terrace construction remains relatively scarce. However, as a form of land use, the suitability evaluation of terrace construction can refer to the theoretical frameworks and technical methods of farmland suitability evaluation. The evaluation of farmland suitability often adopts different evaluation index systems and methods according to the specific land use purpose. The evaluation index systems usually consider natural, ecological, social and economic factors, such as climate, topography, water resources, soil, irrigation conditions, LULC (land use/land cover), infrastructure, population density, GDP, etc. [10–12]. The commonly used evaluation methods include the Delphi, analytic hierarchy process (AHP), analytic network process (ANP), principal component analysis (PCA), entropy weight method (EWM), fuzzy comprehensive evaluation (FCE), fuzzy analytic hierarchy process (FAHP), etc. [13–18]. To achieve the quantitative expression and spatial integration of multiple indicators, and produce accurate visual evaluation results, some scholars have applied GIS technology to evaluate farmland suitability. Specifically, scholars commonly adopt the following scheme: overlaying and summing the weighted raster layers of each indicator to obtain a comprehensive evaluation index, and then classifying the suitability grades [19,20]. This approach has demonstrated significant practical value in precision agriculture management and land use planning.

Some scholars have studied the erosion control and sediment reduction effects of existing terraces in the Loess Plateau by means of experimental observation or model simulation. Experimental observation can accurately record the erosion control and sediment

reduction effects of different terrace systems through field monitoring, but this method has the drawbacks of high input costs, relatively simple surface conditions and limited sample representativeness [21–23]. A few scholars have introduced parameters such as "terrace area ratio" and "sediment reduction amount" to develop models of the relationship between terrace area ratio and sediment reduction, thereby analyzing the sediment reduction effect of terraces at various spatiotemporal scales [24–26]. These model methods have significantly expanded the spatiotemporal scope of research, but they have several limitations, such as insufficient consideration of surface conditions, oversimplified model assumptions, and the inability to reveal the regulatory effect of terrace distribution pattern on sediment reduction. The approach, which combines terrace distribution pattern with soil erosion model simulation (such as the commonly used USLE/RUSLE models), has become a vital tool for evaluating the erosion control and sediment reduction potential of terraces at a regional scale [27]. More broadly, RUSLE-based erosion assessment has also been increasingly integrated with sustainable land-management planning and the evaluation of conservation measures. For example, Rončević et al. [28] combined erosion assessment with prevention measures and socioeconomic investment analysis, while Tričković et al. [29] used RUSLE to compare erosion risk under existing and projected agricultural production structures and further evaluated their ecological and economic effects.

Among available empirical models, the RUSLE has been one of the most widely used tools for estimating long-term average annual soil loss and for supporting regional soil conservation planning, especially when integrated with GIS and remote sensing data [30,31]. Importantly, terrace measures can be incorporated into the RUSLE framework through changes in topographic conditions and, in particular, the support practice factor (P), which is specifically designed to represent the effects of conservation practices such as contouring and terracing on soil erosion [32,33]. Recent studies have further demonstrated that model-based approaches can effectively quantify the contribution of terraces to soil erosion mitigation on the Loess Plateau and other hilly landform regions of China [34,35]. Therefore, although RUSLE mainly estimates sheet and rill erosion rather than gully erosion, it provides a practical and reliable framework for comparing pre- and post-terracing soil loss on sloping farmland and for assessing the sediment reduction potential of terrace construction at a regional scale.

Therefore, the objectives of this study were (1) to preliminarily determine the research area based on the precipitation requirements for dry-farming terrace construction in the Loess Plateau, and to analyze the spatial distribution of the current soil erosion intensity using the RUSLE model in combination with GIS technology; (2) to develop a suitability evaluation index system incorporating 12 influencing factors that cover precipitation, topography, water resources, soil erosion, socioeconomic conditions, etc., and to evaluate the construction suitability and spatial distribution of dry-farming wide terraces on sloping farmland using a multidimensional decision-making framework that includes the analytic hierarchy process (AHP), the fuzzy membership function method, and a comprehensive index model; and (3) to explore the sediment reduction potential of dry-farming wide terraces on sloping farmland based on the suitability classification results and the RUSLE model. This study represents a significant advancement in terrace planning by addressing the limitations of previous studies that predominantly emphasized topography and soil factors. By integrating multiple influencing factors and utilizing a multidimensional decision-making framework, this study provides a novel approach to evaluate terrace construction suitability in semi-arid and semi-humid regions. Moreover, it offers valuable theoretical insights for the construction of dry-farming wide terraces and soil erosion control in the Loess Plateau and other regions with similar environmental conditions.

2. Materials and Methods

2.1. Study Area

The research object of this study is the distribution area of farmland in the Loess Plateau. The Loess Plateau, as one of the most serious areas of soil and water loss in China, is situated in northern China (34° N–40° N, 103° E–114° E) and covers an area of approximately 640,000 km^2 [36]. The geomorphic units of the Loess Plateau are complex, with elevations ranging from 85 to 4885 m. It has a continental monsoon climate, with a mean annual temperature of 8 °C to 14 °C and mean annual precipitation of 120 mm to 760 mm [37]. In the areas north and west of the 400 mm mean annual precipitation isohyet, the natural environment differs markedly from that of the main farming areas. The northwestern part is dominated mainly by sandy land, whereas the southwestern part is characterized mainly by loess tableland-gully landforms. In these areas, cropland is relatively limited, and sloping farmland is less concentrated. By contrast, cropland, especially sloping farmland, is distributed mainly in the areas with mean annual precipitation $\geq$ 400 mm, where existing farmlands and terraces are also concentrated.

According to the spatial distribution characteristics of farmland and the precipitation requirement (mean annual precipitation $\geq$ 400 mm) specified in the 2021 guidelines of the Ministry of Water Resources of China for dry-farming terrace construction in the Loess Plateau, this study preliminarily determined the research area. As shown in Figure 1, the final research area lies to the east and south of the 400 mm mean annual precipitation isohyet. Although a limited number of existing terraces may occur in areas with mean annual precipitation < 400 mm, these areas generally contain much less cropland and are not the main distribution zone of sloping farmland considered in this study.

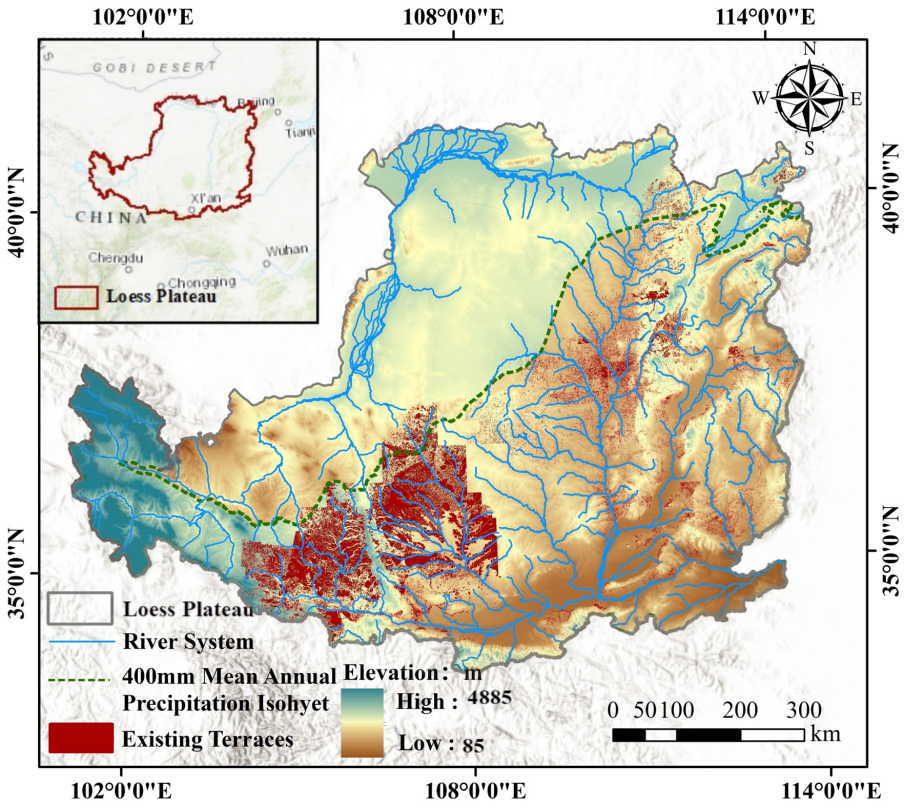


Figure 1. Location of the Loess Plateau and distribution of the existing terrace.

The research area covers approximately 405.24 × 10^3 km^2, accounting for about 63% of the total area of the Loess Plateau, and spans parts of seven provinces: Shanxi,

Shaanxi, Gansu, Qinghai, Henan, Ningxia Hui Autonomous Region, and Inner Mongolia Autonomous Region. In this area, the dominant geomorphic types are loess hilly-gully and loess plateau-gully landforms, characterized by fragmented terrain, deeply incised gullies, and steep slopes. The mean annual precipitation ranges from 400 mm to 760 mm, generally increasing from the northwest to the southeast [37]. The dominant soil type is yellow loess, which is loose and porous (WRB classification). Based on the statistics of this study, the main land use types are cultivated land (with sloping farmland accounting for a large proportion), grassland, and forestland, and vegetation coverage is mainly below the moderate level. Owing to the geographical constraints, the region experiences severe soil erosion [38]. These environmental characteristics demonstrate the necessity and potential feasibility of wide terrace construction on sloping farmland in the research area, and, therefore, provide an appropriate basis for evaluating the construction suitability and sediment reduction potential of dry-farming wide terraces on sloping farmland.

2.2. Data Sources

The datasets included daily precipitation, DEM, geomorphic type, land use, NDVI, soil-related data, river systems, terrace distribution, and socioeconomic data such as population density, transportation networks, and village/town centers. The sources, temporal coverage, and spatial resolution of all datasets are summarized in Table 1. The datasets were obtained from authoritative institutions and data platforms (Table 1) and have been widely used in regional environmental studies [39–44], thus providing reliable support for the present analysis.

Input data were classified into dynamic and relatively static factors based on the frequency and magnitude of their temporal variations. Dynamic factors mainly included daily precipitation, NDVI, land use, and population density, whereas relatively static factors included DEM, geomorphic type, soil texture, soil organic carbon, river systems, transportation networks, village/town centers, and terrace distribution. Given that relatively static factors change slowly over short- to medium-term periods across the Loess Plateau, they can be analyzed within the same temporal framework (2016–2020) as dynamic factors. Therefore, despite the datasets spanning different years, such temporal inconsistency is unlikely to substantially alter the main regional suitability pattern, although it may introduce some uncertainty in local details.

In this study, daily precipitation records from 79 meteorological stations during 1990–2020 were first used to calculate annual and multiyear mean precipitation, as well as the rainfall erosivity factor. Multiyear mean spatial distributions of these variables were then generated by inverse distance weighting (IDW) interpolation. DEM data were processed to derive topographic variables, including elevation, slope, slope aspect, and the LS factor for the RUSLE model. Land use data were mainly used to determine the P factor for the RUSLE model. Soil texture and soil organic carbon data were used to calculate the K factor, and geomorphic type, river systems, transportation networks, village/town centers, and population density were further used to derive the corresponding suitability evaluation indicators.

For vegetation conditions, annual composite NDVI data from 2016 to 2020 were averaged to obtain a multiyear mean NDVI, which was further used to calculate the vegetation cover management factor (C). The terrace distribution dataset was employed as an external spatial terrace inventory to characterize the existing terrace pattern and to support plausibility checking and post hoc interpretation of the modeled suitability results through spatial overlay analysis, rather than serving as a direct model input.

To ensure consistency with the spatial resolution of the DEM, all raster datasets were resampled to 12.5 × 12.5 m grids and assigned a unified projection coordinate system

(Xian_1980_GK_CM_111E). This resampling was performed for spatial harmonization only and did not improve the intrinsic resolution or accuracy of originally coarser datasets. At the regional scale of the study, the 90 m soil organic carbon data and the 1000 m population density data still provide sufficiently high precision for representing broad spatial patterns, although some uncertainty may remain near fine-scale spatial boundaries after resampling.

Table 1. Data sources and characteristics used in this study.

Data Name	Data Source	Spatial Resolution	Temporal Period
Daily precipitation	China Meteorological Administration (http://data.cma.cn/)	79 Station data	Daily, 1990–2020
DEM	NASA Earthdata (https://search.earthdata.nasa.gov/search)	12.5 m	2007
Geomorphic type	Data Center for Resources and Environmental Sciences, Chinese Academy of Sciences (RESDC) (https://www.resdc.cn/)	30 m	2020
Soil texture	Data Center for Resources and Environmental Sciences, Chinese Academy of Sciences (RESDC) (https://www.resdc.cn/)	30 m	2020
Land use	Data Center for Resources and Environmental Sciences, Chinese Academy of Sciences (RESDC) (https://www.resdc.cn/)	30 m	2020
NDVI	Institute of Geographic Sciences and Natural Resources Research, Chinese Academy of Sciences (https://www.igsnrr.cas.cn/)	30 m	Annual composite/multiyear mean, 2016–2020
Terrace distribution	National Earth System Science Data Center (http://www.geodata.cn)	30 m	2015
Soil organic carbon	National Earth System Science Data Center (http://www.geodata.cn/)	90 m	2010–2018
River system	National Earth System Science Data Center (http://www.geodata.cn/)	Vector data	Static/latest available
Transportation network	National Earth System Science Data Center (http://www.geodata.cn/)	Vector data	2000
Village/town centers	National Earth System Science Data Center (http://www.geodata.cn/)	Vector data	2000
Population density	ORNL, U.S. Department of Energy (LandScan) (https://www.ornl.gov/)	1000 m	2020

2.3. Methods

2.3.1. Soil Erosion Modulus Calculation

To characterize the soil erosion intensity of sloping farmland in the research area, the Revised Universal Soil Loss Equation (RUSLE) model was applied to estimate the soil erosion modulus under baseline conditions during 2016–2020 and under construction scenarios of dry-farming wide terraces. The use of RUSLE was considered appropriate for this study because the research focuses on regional-scale comparison of soil erosion

intensity on sloping farmland and on scenario-based comparison before and after wide terrace construction. On cultivated slopes, the dominant erosion forms are mainly sheet and rill erosion, whereas large gully erosion is generally less likely to develop under annual tillage and routine agricultural management. Therefore, although RUSLE does not fully capture gully-dominated erosion processes, it is still suitable for the present purpose. The formula is as follows:

$$A = R \times K \times L \times S \times C \times P \quad (1)$$

where A is the annual average soil loss per unit area (t/(hm^2·a)); R is the rainfall erosivity factor (MJ·mm/(hm^2·h·a)); K is the soil erodibility factor (t·hm^2·h/(hm^2·MJ·mm)); L and S are the slope length and slope steepness factors (dimensionless); C is the cover management factor (dimensionless); and P is the soil conservation practice factor (dimensionless). The calculated soil erosion modulus was classified according to China's SL190–2007 standard (approved by the Ministry of Water Resources of China, 2007) into six intensity grades: micro ($\leq$500 t·km^{-2}·a^{-1}), slight (500–2500 t·km^{-2}·a^{-1}), moderate (2500–5000 t·km^{-2}·a^{-1}), strong (5000–8000 t·km^{-2}·a^{-1}), very strong (8000–15,000 t·km^{-2}·a^{-1}), and severe (>15,000 t·km^{-2}·a^{-1}).

① Rainfall erosivity factor (R)

The rainfall erosivity was calculated using the formula proposed by Zhang et al. [45]. The formula is as follows:

$$R = \alpha\left(\sum_{j=1}^{k} pd\right)^{\beta} \quad (2)$$

$$\alpha = 21.586\beta^{-7.1891} \quad (3)$$

$$\beta = 0.8363 + \left(\frac{18.144}{P_{d12}}\right) + \left(\frac{24.455}{P_{y12}}\right) \quad (4)$$

where R is the half-monthly rainfall erosivity (MJ·mm/(hm^2·h·a)); k is the number of days in the half-monthly period (d); P_d is the daily rainfall (mm); α and β are regression coefficients; P_{d12} is the average daily erosive rainfall (mm) with daily rainfall $\geq$ 12 mm; and P_{y12} is the average annual erosive rainfall (mm) with daily rainfall $\geq$ 12 mm.

For rainfall erosivity processing, daily precipitation data from 79 meteorological stations on the Loess Plateau were first used to calculate annual rainfall erosivity at each station for 1990–2020. The station-based annual values were then averaged to obtain the multiyear mean rainfall erosivity for the target period, and the corresponding spatial surface was generated in ArcGIS10.8 by interpolation. After comparing the interpolation performance of commonly used methods, IDW was selected for this study because it yielded a relatively stable spatial pattern and satisfactory interpolation accuracy for the station distribution of the study area. The final 2016–2020 mean rainfall erosivity raster of the research area was then derived.

② Soil erodibility factor (K)

The soil erodibility factor of each soil type in the research area was calculated using the method of EPIC model [46]. The calculation formula is as follows:

$$K = \left\{0.2 + 0.3_{exp}\left[-0.0256S_a\left(1 - \frac{S_j}{100}\right)\right]\right\}\left(\frac{S_j}{C_j+S_j}\right)^{0.3}\left[1 - \frac{0.25O}{O+exp(3.72+2.95O)}\right]\left[1 - \frac{0.7S_n}{S_n+exp(-5.51+22.9S_nO)}\right] \times 0.1317 \quad (5)$$

where $S_n = 1 - S_a/100$; S_a is the sand content (%) (0.05–2 mm); S_j is the silt content (%) (0.002–0.05 mm); C_j is the clay content (%) (<0.002 mm); O is the organic carbon content (%); and 0.1317 is the conversion factor from the U.S. unit to the international unit.

The sand, silt, and clay contents were obtained from the soil texture dataset, and the organic carbon content was obtained from the soil organic carbon dataset. Before

calculation, these layers were projected to the same coordinate system and aligned to the same raster framework used in this study. The required variables were then extracted on a cell-by-cell basis for K-factor calculation. No additional unit conversion was required beyond the conversion coefficient already included in Equation (5).

③ Slope length factor and slope steepness factor (*LS*)

Based on the DEM with a spatial resolution of 12.5 m, the LS factors for the research area were calculated using the formulas proposed by Liu et al. [47]. The formulas are as follows:

$$L = (\lambda / 22.1)^m \quad m = \begin{cases} 0.2 & \theta < 1^\circ \\ 0.3 & 1^\circ \le \theta < 3^\circ \\ 0.4 & 3^\circ \le \theta < 5^\circ \\ 0.5 & \theta \ge 5^\circ \end{cases} \tag{6}$$

$$S = \begin{cases} 10.8\sin\theta + 0.036 & \theta < 5^\circ \\ 16.8\sin\theta - 0.5 & 5^\circ \le \theta < 10^\circ \\ 21.9\sin\theta - 0.96 & \theta \ge 10^\circ \end{cases} \tag{7}$$

where L and S are the slope length factor and slope steepness factor, respectively; λ is the slope length (m); 22.1 is the standard slope length for the plot; m is the slope length exponent; and θ is the slope (°).

In GIS processing, slope and flow-related terrain attributes were first derived from the 12.5 m DEM. Slope length was then obtained through terrain and hydrological analysis based on DEM-derived flow path information, and the resulting slope length and slope steepness layers were subsequently used to calculate the LS factor.

④ Cover management factor (*C*)

The *C* factor was calculated based on the average *NDVI* during 2016–2020. Many scholars have established relationships between *NDVI* and *C*, and this study adopted the relationship formula proposed by Van der Knijff et al. [48] to calculate the cover management factor. The formula is as follows:

$$C = e^{(-\alpha(NDVI)/\ (\beta - NDVI))} \tag{8}$$

where *C* is the cover management factor; the parameters α and β are dimensionless, with α = 2 and β = 1; and *NDVI* is the Normalized Difference Vegetation Index.

A multiyear average NDVI for 2016–2020 was used instead of annual NDVI because this study aimed to represent the mean soil erosion condition of the same multiyear period and to reduce the influence of short-term interannual fluctuations in vegetation cover. This treatment is consistent with the regional-scale objective of the study, although it may smooth some year-to-year variability in vegetation conditions and, therefore, introduce limited uncertainty into the erosion estimates.

⑤ Soil conservation practice factor (*P*)

The *p* values were determined based on land use types of 2020 and previous research [49,50]. The *p* values were as follows: cultivated land, 0.35; forestland, 0.23; high-coverage grassland, 0.15; medium-coverage grassland, 0.24; low-coverage grassland, 0.45; built-up land, 0.9; water, 1; unused land, 1; and dry-farming wide terraces, 0.22.

These *p* values were generalized from published studies and assigned by land use category in order to provide an operational regional-scale representation of conservation practices. Such treatment may simplify the actual variability of conservation management across the Loess Plateau and, therefore, constitutes a source of uncertainty, especially for cultivated land and terrace-related scenarios. The *p* value of 0.22 for dry-farming wide

terraces was selected as a generalized scenario parameter based mainly on previous studies on terrace conservation effects in the Loess Plateau and related hilly regions, and it was used here to represent the expected reduction in soil erosion under a standardized wide terrace construction scenario rather than a site-specific measured value.

2.3.2. Suitability Evaluation Method

(1) Determination of indicator weights and fuzzy membership degrees

A combined AHP–fuzzy membership framework was adopted to evaluate the construction suitability of dry-farming wide terraces. This approach was used because terrace suitability depends both on the relative importance of multiple indicators and on the nonlinear relationships between indicator values and suitability levels. AHP was applied to determine indicator weights, whereas fuzzy membership functions were used to standardize heterogeneous indicators into comparable suitability scores ranging from 0 to 1.

Based on the characteristics of precipitation, topography, water resources, soil erosion, and socioeconomic conditions on the Loess Plateau, and in line with relevant policy documents on dry-farming terrace construction and soil and water conservation in the Yellow River Basin, a suitability evaluation index system was developed. Twelve indicators were selected (Table 1): slope, elevation, slope aspect, landform type, annual precipitation, distance to water sources, soil texture, soil organic matter, soil erosion modulus, road accessibility, accessibility to village centers, and population density. These indicators were chosen because they represent the main constraints on terrace construction from four aspects: topographic and geomorphological conditions, water-resource conditions, soil and erosion conditions, and socioeconomic accessibility.

The weights of the selected indicators were determined using the AHP method (Table 2) [51,52]. The indicators were first organized into a hierarchical structure, and judgment matrices were then constructed through pairwise comparison based on the Delphi method and expert consultation. The maximum eigenvalue and corresponding single-ranking weights of each matrix were calculated, followed by consistency tests. All judgment matrices passed the consistency test, with CR values lower than 0.10. The overall ranking consistency ratio was 0.0373, indicating acceptable internal consistency of the expert judgments. It should be noted that the CR test confirms the internal consistency of the AHP judgment matrices, but does not by itself establish the external validity of the weighting scheme, which still depends on the appropriateness of the selected indicators and assumptions.

Table 2. Weights of the evaluation indicators of construction suitability of dry-farming wide terraces.

Objective Layer A	Criterion Layer B	Weight B_i	Indicator Layer C	Weight C_j	Combined Weight $\sum B_i C_j$
Evaluation of construction suitability of dry-farming wide terraces (A)	Topography and landform factors (B_1)	0.5104	Slope (C_1)	0.6127	0.3127
			Elevation (C_2)	0.0876	0.0447
			Slope aspect (C_3)	0.1920	0.0980
			Landform type (C_4)	0.1077	0.0550
	Water resource factors (B_2)	0.1040	Annual precipitation (C_5)	0.3333	0.0347
			Distance to water source (C_6)	0.6667	0.0693
	Soil factors (B_3)	0.1594	Soil texture (C_7)	0.1929	0.0307
			Soil organic matter (C_8)	0.1061	0.0169
			Soil erosion modulus (C_9)	0.7010	0.1117
	Socioeconomic factors (B_4)	0.2262	Accessibility to road (C_{10})	0.6250	0.1414
			Accessibility to village/town center (C_{11})	0.2385	0.0539
			Population density (C12)	0.1365	0.0309

According to fuzzy mathematics, the relationships between the selected indicators and terrace construction suitability were classified into four types of membership functions: upper-limit, peak, linear, and conceptual. Numerical indicators were represented by upper-limit, peak, or linear functions, and the corresponding parameters are listed in Table 3. Numerical indicators were represented by upper-limit, peak, or linear functions, and the corresponding parameters are listed in Table 3. Conceptual indicators, including landform type, soil texture, and slope aspect, were assigned membership degrees according to category-based suitability differences, with reference to previous studies and expert consultation (Table 4). These assigned membership values were, therefore, not based on expert consultation alone, but were checked against published studies and adapted to the environmental and engineering conditions of the Loess Plateau.

Table 3. Membership functions for numeric evaluation indicators.

Function Type	Evaluation Indicator	Membership Function	a	b	c	U_1	U_2
Peak-shaped type	Slope	$Y = 1/[1 + a \times (u - c)^2]$	0.028488		11.49376	5	25
Upper-restricted type	Soil organic matter	$Y = 1/[1 + a \times (u - c)^2]$	0.017246		23.0947	0.25	23.0947
Upper-restricted type	Population density	$Y = 1/[1 + a \times (u - c)^2]$	0.00032		119.1629	0	119.1629
Linear type	Precipitation	$Y = b + a \times u$	0.001905	−0.533333		400	800
Linear type	Soil erosion modulus	$Y = b + a \times u$	0.014815	0.303704		100	5000
Negative linear type	Elevation	$Y = b - a \times u$	−0.000367	1.24681		700	3150
Negative linear type	Accessibility to road	$Y = b - a \times u$	−0.000064	1.16		2600	16,000
Negative linear type	Distance to water source	$Y = b - a \times u$	−0.000068	1.190164		2900	16,000
Negative linear type	Accessibility to village/town center	$Y = b - a \times u$	−0.0004	1.28		8000	29,000

Table 4. Membership degrees for conceptual evaluation indicators.

Evaluation Indicator	Description and Membership Degree						
Slope aspect	Description	Flat Land	South-facing	Semi-south-facing	North-facing	Semi-north-facing	
	Membership degree	0.8	1	0.9	0.6	0.8	
Landform type	Description	Plain	Terrace	Hillock	Low mountain	Middle mountain	High mountain
	Membership degree	1	0.9	0.8	0.7	0.5	0.2
Soil texture	Description	Loam	Sandy soil	Clay soil			
	Membership degree	1	0.6	0.7			

For the slope factor, the optimal range for terrace construction was set to 5–25° [53,54], and a peak-shaped membership function was adopted (Table 3). This setting was used because slopes below 5° generally have limited need for terrace transformation, whereas slopes above 25° are generally unsuitable for terrace construction under existing policy and

engineering standards. Therefore, slope suitability increases to the appropriate construction interval and then decreases beyond the upper threshold, which is consistent with the peak-shaped function.

The AHP consistency test, membership-function design, and expert-based assignment of membership degrees were used as components of model construction to generate the final suitability scores and classes, rather than as independent result outputs. At the same time, the use of AHP, Delphi consultation, and expert-based membership assignment introduces a certain degree of subjectivity into the suitability assessment. The relative-importance scoring in the AHP procedure and the assignment of fuzzy membership values were both based to some extent on expert knowledge and experience, which introduces a certain degree of subjectivity into the suitability evaluation. These two steps directly influence the indicator weights and suitability scores, and, therefore, affect the final ISI values and the classification results. No formal sensitivity analysis of indicator weights or membership values was conducted in this study. Therefore, changes in weights or membership assignments may affect the final suitability map, especially near suitability-class boundaries, and this should be regarded as a limitation.

To examine the plausibility of the modeled suitability results, spatial overlay analysis was conducted between the predicted suitable classes (highly suitable, suitable, and barely suitable areas) and the existing terrace distribution, and the corresponding overlap areas and overlap ratios were calculated.

(2) Calculation and classification of the Integrated Suitability Index (ISI)

The Integrated Suitability Index (ISI) for each evaluation unit within the research area was calculated using a weighted model [55]. The formula is as follows:

$$ISI = \sum F_i \times C_i \ (i = 1, 2, 3, \ldots n) \quad (9)$$

where F_i is the evaluation value of the i-th indicator, and C_i is the combined weight of the i-th indicator. Based on ISI of each evaluation unit and the cumulative frequency curve, the following four grades of construction suitability of dry-farming wide terraces were defined: highly suitable (ISI > 0.7, T_1), suitable (0.6 < ISI $\leq$ 0.7, T_2), barely suitable (0.5 < ISI $\leq$ 0.6, T_3), and unsuitable (ISI $\leq$ 0.5, T_4).

In this study, the areas of T_1, T_2, T_3, and T_4 were calculated for the whole research area, as well as for each province and prefecture-level city within it. According to the ranking of the total area of highly suitable and suitable areas (T_1 + T_2), as well as the total area of highly suitable, suitable, and barely suitable areas (T_1 + T_2 + T_3), for each province and prefecture-level city, the construction intensity of each province and prefecture-level city was determined under the two scenarios.

3. Results

3.1. Current Soil Erosion Intensity in the Research Area

3.1.1. Spatial Variability of RUSLE Model Factors

The spatial distributions of the RUSLE model factors in the research area during 2016–2020 are shown in Figure 2. The rainfall erosivity factor (R) spatially increased from the northwest to the southeast, with an average of 1861 MJ·mm/(hm^2·h·a). The soil erodibility factor (K) generally increased from the northern and southern margins to the central part, with an average value of 0.0350 t·hm^2·h/(hm^2·MJ·mm). The average slope of the research area was 16°, and the areas with slopes of 5–25° accounted for 61.3%. The LS factor ranged from 0 to 72, with an average value of 5.93. LS showed a spatial pattern similar to that of slope. Lower LS values were found in most of the southern part, the northern margin and river valleys, whereas higher values occurred in the southern

margin, the eastern margin and most of the western part. The average *NDVI* was 0.55, and *NDVI* values were mainly concentrated in the range of 0.4–0.8, accounting for 84.7%. The *C* factor decreased from northwest to southeast, with an average value of 0.129. It was closely associated with *NDVI*, with higher *NDVI* values generally corresponding to lower *C* values. Higher *C* values were mainly concentrated in the western part, the northern margin, river valleys, and residential areas, whereas lower values were mainly distributed in forestland and grassland areas. The main land use types were cultivated land (accounting for 35.7%), grassland (accounting for 21.0%) and forestland (accounting for 37.0%). The spatial distribution of the *P* factor varied with land use pattern, and its higher values were mainly distributed in parts of the southern, western and northern areas.

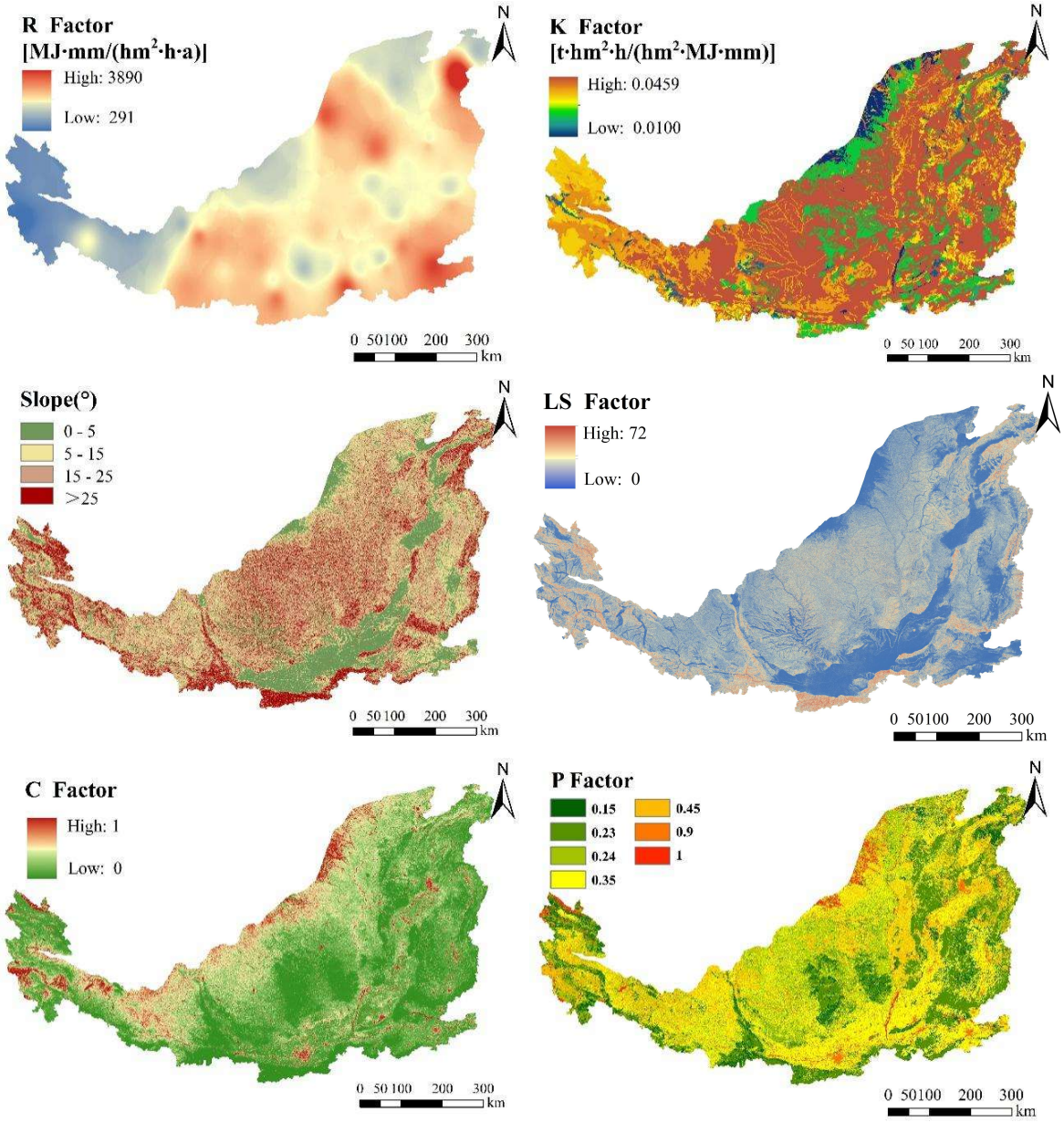


Figure 2. Spatial distributions of RUSLE model factors in the research area during 2016–2020.

3.1.2. Soil Erosion Intensity

The average soil erosion modulus in the research area during 2016–2020 was 1484 $t \cdot km^{-2} \cdot a^{-1}$. The areas of micro, slight, moderate, strong, very strong, and severe erosion were 207.84 × 10^3 km^2, 125.08 × 10^3 km^2, 43.85 × 10^3 km^2, 17.06 × 10^3 km^2,

8.34 × 10^3 km^2, and 2.70 × 10^3 km^2, respectively, accounting for 51.3%, 30.9%, 10.8%, 4.2%, 2.1%, and 0.7% of the total research area. Overall, micro and slight erosion were the dominant erosion types, accounting for 82.2% of the research area. Micro and slight erosion were widely concentrated in the eastern and southern parts of the research area, whereas moderate to severe erosion was mainly distributed in the western and northern parts, as well as in river valleys and gullies.

In terms of the soil erosion intensity of each province within the research area (Figure 3), Ningxia Hui Autonomous Region and Gansu Province exhibited the most severe erosion, with moderate to severe erosion accounting for 37.2% and 30.1% of their respective evaluated areas. In contrast, Henan Province demonstrated the lightest erosion, with micro to slight erosion covering 93.3% of its evaluated area. Additionally, the area proportions of micro to slight erosion in the Inner Mongolia Autonomous Region, Shanxi Province, Shaanxi Province, and Qinghai Province were similar, accounting for 83.7%, 86.0%, 84.2%, and 86.8%, respectively.

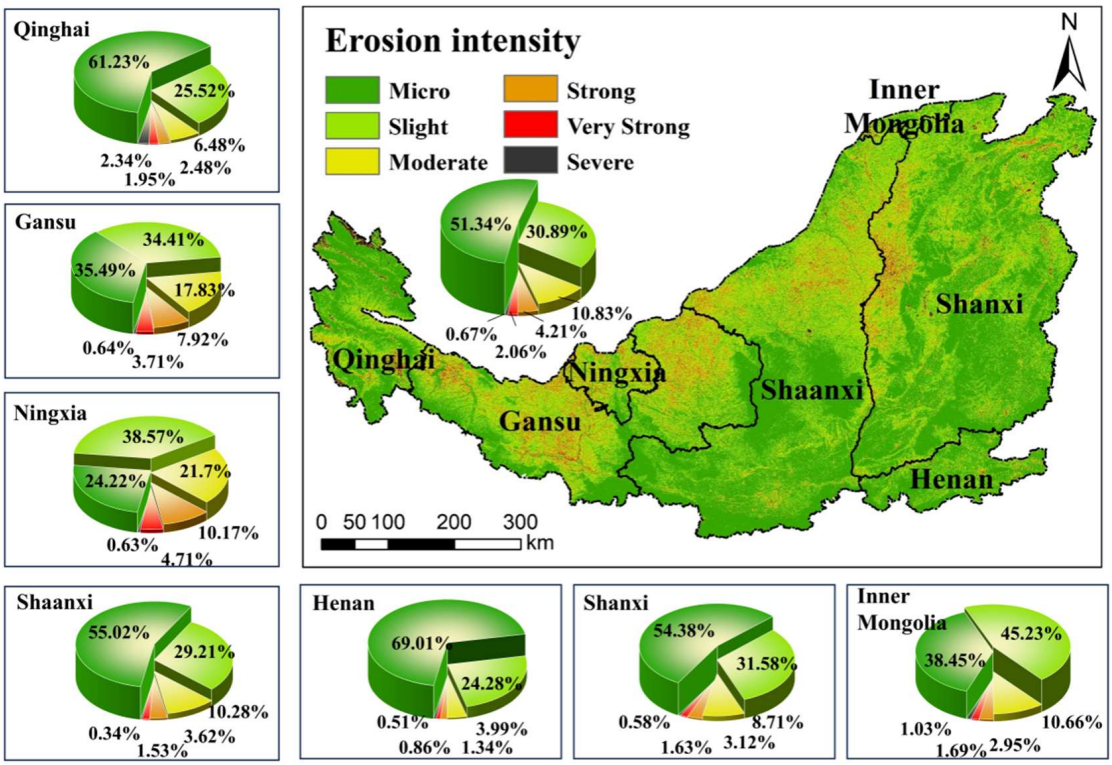


Figure 3. Spatial distribution of soil erosion intensity in the research area during 2016–2020.

3.2. Construction Suitability and Spatial Distribution of Dry-Farming Wide Terraces

(1) Classification of construction suitability

The ISI of the construction suitability of dry-farming wide terraces in the research area ranged from 0.13 to 0.97, excluding the non-evaluation areas with slopes lower than 5° or greater than 25° and the non-cultivated areas. High ISI values were mainly distributed in the central, western and southeastern areas, whereas low values were mainly distributed in the western and northern areas. The areas of highly suitable construction (T_1), suitable construction (T_2), barely suitable construction (T_3) and unsuitable construction (T_4) were 30,578.19 km^2, 29,311.69 km^2, 17,300.60 km^2 and 5587.52 km^2, respectively, accounting for 7.5%, 7.2%, 4.3% and 1.4% of the total research area (Figure 4).

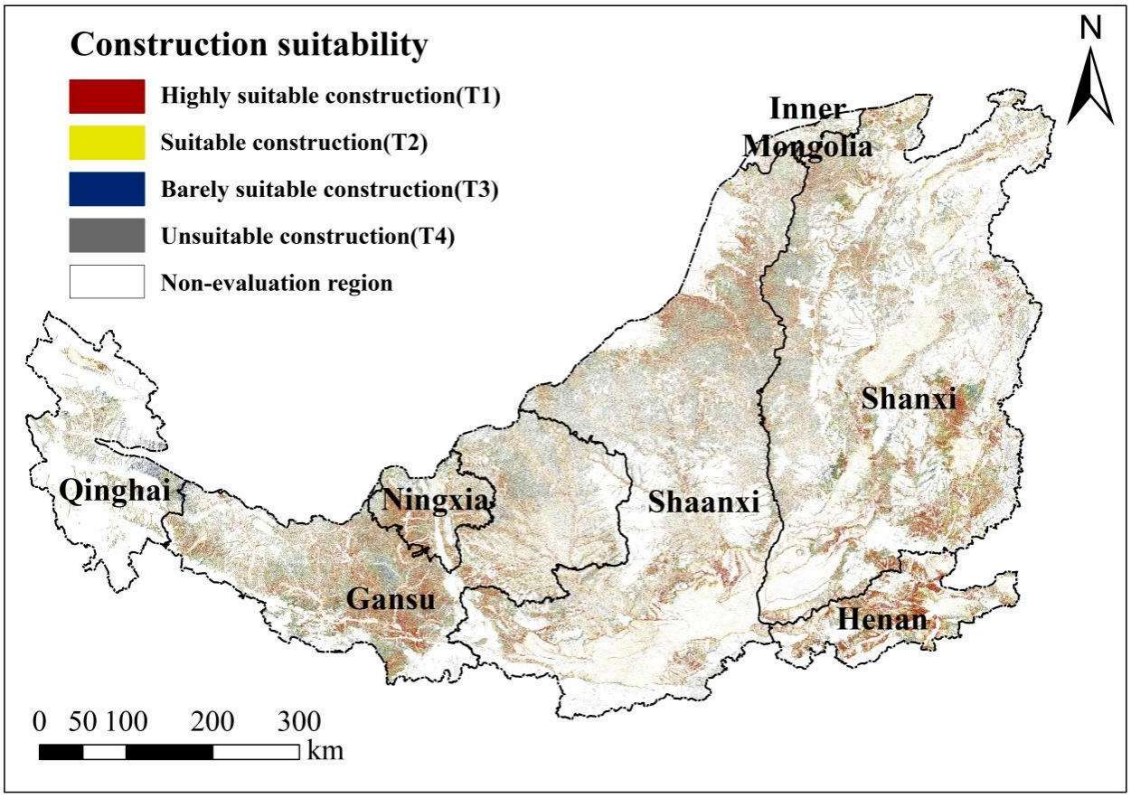


Figure 4. Spatial distribution of construction suitability of dry-farming wide terraces.

The total area of existing terraces in the research area is 51,489.88 km^2. Among this, Gansu Province has the largest terrace area, covering 29,511.12 km^2, which accounts for 57.3% of the total. Other provinces and regions include Shanxi Province (9616.5 km^2, 18.7%), Shaanxi Province (7379.34 km^2, 14.3%), and Ningxia Hui Autonomous Region (4744.50 km^2, 9.2%).

This comparison indicates that the modeled suitability results are spatially consistent with the existing terrace pattern to a certain extent, and, therefore, provides partial support for the rationality of the suitability evaluation (Figure 5). Specifically, the overlapping areas of highly suitable, suitable and barely suitable areas with existing terrace area were 8041.13 km^2, 7146.76 km^2 and 4251.66 km^2, respectively, and the overlap ratios were 15.6%, 13.9% and 8.3%, respectively. Consequently, the cumulative overlap ratios of (T_1 + T_2) and (T_1 + T_2 + T_3) with existing terraces were 29.5% and 37.8%, respectively. The overlapping areas were mainly concentrated in Gansu Province and Ningxia Hui Autonomous Region.

To assess the potential impact of terrace construction on soil erosion reduction, this study considered two construction scenarios:

1. T_1 + T_2 scenario: This scenario involves constructing terraces in the areas identified as highly suitable (T_1) and suitable (T_2) for terrace construction. These regions are characterized by optimal conditions for dry-farming terraces and are expected to yield significant reductions in soil erosion due to their capacity to sustain terraces with minimal landscape modification.
2. T_1 + T_2 + T_3 scenario: This scenario expands construction to include barely suitable (T_3) areas in addition to the highly suitable (T_1) and suitable (T_2) areas. Although the T_3 areas are less ideal for terrace construction, they are still feasible for implementation. Expanding to these regions is expected to provide further benefits for soil erosion reduction, though with a less pronounced effect compared to the T_1 + T_2 scenario.

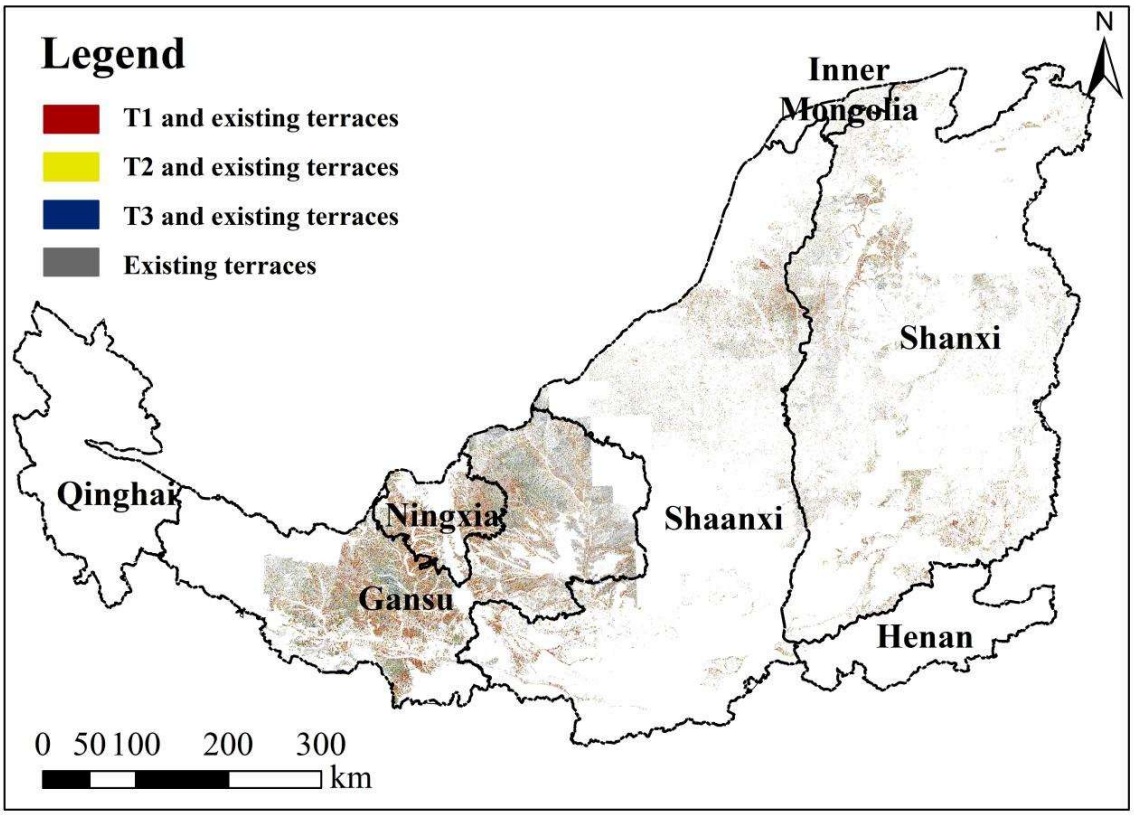


Figure 5. Overlapping areas between the evaluation results of construction suitability and existing terraces in the research area.

(2) Spatial distribution of construction suitability grade

Slope, transportation convenience and soil erosion intensity were the key influencing factors for construction suitability of wide terraces (Table 1). The highly suitable area was concentrated in hilly regions with slopes lower than 15°, convenient transportation, proximity to water sources, high accessibility to villages and towns, high soil fertility and more rainfall, but severe soil erosion. The suitable, barely suitable and unsuitable areas exhibited successively increased slopes, diminished accessibility to roads, water sources and villages/towns, reduced rainfall, and a declining trend in soil erosion intensity.

The distribution of construction suitability across provinces and prefecture-level cities in the research area is shown in Figure 4 and Table 5. Shanxi Province had the largest area in each construction suitability grade. Specifically, the areas classified as highly suitable, suitable, barely suitable, and unsuitable accounted for 33.4%, 35%, 32.6%, and 32.8% of the total area, respectively. Shaanxi and Gansu Provinces ranked second, while the Inner Mongolia Autonomous Region had the smallest areas for each suitability grade. The area of each construction suitability grade in Shaanxi Province and Gansu Province ranked second, while that in the Inner Mongolia Autonomous Region was the smallest. In terms of suitability grade and construction intensity, the top three provinces were Shanxi, Shaanxi and Gansu, and the top three prefecture-level cities were Yulin, Yan'an and Qingyang.

3.3. Sediment Reduction Potential of Dry-Farming Wide Terraces

Based on the evaluation results of construction suitability, two assumed construction scenarios of dry-farming wide terraces were defined for the research area: (1) construction of highly suitable and suitable areas (T_1 + T_2), and (2) construction of highly suitable, suitable and barely suitable areas (T_1 + T_2 + T_3). Under the T_1+T_2 construction scenario, the area of sloping farmland that could potentially be converted to wide terraces would be

59.89 × 10^3 km^2, including 30.58 × 10^3 km^2 of highly suitable areas and 29.31 × 10^3 km^2 of suitable areas. Under the T_1 + T_2 + T_3 scenario, the corresponding area would increase to 77.19 × 10^3 km^2, including an additional 17.30 × 10^3 km^2 of barely suitable areas.

Table 5. Construction area of dry-farming wide terraces in each province in the research area.

Province	Prefecture-Level City	Highly Suitable		Suitable		Barely Suitable		Unsuitable	
		Area (km^2)	Proportion (%)	Area (km^2)	Proportion (%)	Area (km^2)	Proportion (%)	Area (km^2)	Proportion (%)
Shanxi	Taiyuan	281.85	0.9	352.30	1.2	248.94	1.4	86.27	1.5
	Datong	229.00	0.8	285.10	1.0	146.64	0.9	46.80	0.8
	Yangquan	264.58	0.9	236.05	0.8	129.71	0.8	45.49	0.8
	Changzhi	1470.42	4.8	1398.10	4.8	656.20	3.8	240.57	4.3
	Jincheng	1195.47	3.9	893.21	3.1	344.04	2.0	89.26	1.6
	Shuozhou	352.16	1.2	472.77	1.6	244.51	1.4	60.21	1.1
	Jinzhong	742.85	2.4	829.46	2.8	462.27	2.7	147.80	2.7
	Yuncheng	939.78	3.1	823.56	2.8	367.13	2.1	88.73	1.6
	Xinzhou	1768.26	5.8	1737.27	5.9	902.90	5.2	276.24	4.9
	Linfen	1459.19	4.8	1599.63	5.5	1034.79	6.0	335.55	6.0
	Lvliang	1504.98	4.9	1626.77	5.6	1108.32	6.4	415.24	7.4
Inner Mongolia	Hohhot	36.44	0.1	74.14	0.3	54.11	0.3	16.26	0.3
	Ordos	173.89	0.6	130.61	0.5	52.12	0.3	6.02	0.11
Henan	Zhengzhou	175.99	0.6	154.49	0.5	62.31	0.4	11.00	0.2
	Luoyang	1345.40	4.4	895.90	3.1	273.23	1.6	34.84	0.6
	Sanmenxia	802.06	2.6	557.18	1.9	206.19	1.2	36.71	0.7
	Jiyuan	237.74	0.8	146.78	0.5	34.70	0.2	1.67	0.0
Shaanxi	Xi'an	311.66	1.0	300.93	1.0	117.19	0.7	59.40	1.1
	Tongchuan	453.04	1.5	343.06	1.2	167.65	1.0	19.99	0.4
	Baoji	862.10	2.8	726.07	2.5	413.91	2.4	99.93	1.8
	Xianyang	644.88	2.1	705.50	2.4	272.76	1.6	21.91	0.4
	Weinan	827.28	2.7	674.72	2.3	216.26	1.3	53.57	1.0
	Yan'an	1799.14	5.9	2014.80	6.9	1725.73	10.0	644.20	11.5
	Yulin	3450.55	11.3	3124.13	10.7	1997.31	11.5	582.99	10.4
Gansu	Lanzhou	28.42	0.1	52.73	0.2	44.26	0.3	13.79	0.3
	Baiyin	303.03	0.1	276.90	0.9	185.32	1.1	38.15	0.7
	Tianshui	1995.16	6.5	1474.58	5.0	839.18	4.9	186.68	3.3
	Pingliang	1434.64	4.7	1201.15	4.1	612.65	3.5	130.36	2.3
	Qingyang	1722.53	5.6	1904.02	6.5	1351.65	7.8	483.42	8.7
	Dingxi	1392.31	4.6	1557.42	5.3	1073.70	6.2	386.40	6.9
	Linxia	472.74	1.6	592.79	2.0	455.94	2.6	175.01	3.1
Qinghai	Xining	180.46	0.6	279.21	1.0	220.54	1.3	87.99	1.6
	Haidong	160.84	0.5	454.35	1.6	524.54	3.0	472.10	8.5
	Haibei	59.61	0.2	96.89	0.3	48.29	0.3	10.30	0.2
	Huangnan	22.95	0.1	30.74	0.1	19.30	0.1	4.30	0.1
	Hainan	14.15	0.1	34.35	0.1	20.99	0.1	9.91	0.2
Ningxia	Guyuan	1446.54	4.7	1195.42	4.1	609.18	3.5	131.98	2.4
	Zhongwei	16.10	0.1	58.61	0.2	56.13	0.3	36.47	0.7
	Total	30,578.19	100	29,311.69	100	17,300.60	100	5587.52	100

The soil erosion intensity (Figure 6, Table 6) and sediment reduction potential under the two construction scenarios of dry-farming wide terraces in the research area were then evaluated. The current average soil erosion modulus was 1484 $t \cdot km^{-2} \cdot a^{-1}$. If T_1 + T_2 or T_1 + T_2 + T_3 can be implemented, the average soil erosion modulus will be reduced to 1238 $t \cdot km^{-2} \cdot a^{-1}$ or 1157 $t \cdot km^{-2} \cdot a^{-1}$, representing reductions of 16.6% or 22.0%, respectively. Overall, the T_1 + T_2 + T_3 scenario would produce a greater improvement in soil erosion control than the T_1 + T_2 scenario.

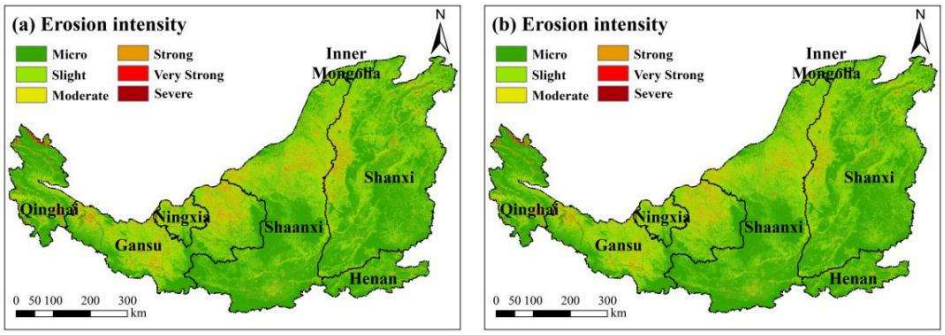


Figure 6. Spatial distributions of soil erosion intensity under two construction scenarios of dry-farming wide terraces: (**a**) construction of highly suitable and suitable areas, and (**b**) construction of highly suitable, suitable and barely suitable areas.

Table 6. Area of soil erosion intensity under the two construction scenarios of dry-farming wide terraces.

Construction Scheme	Micro Erosion		Slight Erosion		Moderate Erosion		Strong Erosion		Very Strong Erosion		Severe Erosion	
	Area (10^3 km^2)	Proportion (%)	Area (10^3 km^2)	Proportion (%)	Area (10^3 km^2)	Proportion (%)	Area (10^3 km^2)	Proportion (%)	Area (10^3 km^2)	Proportion (%)	Area (10^3 km^2)	Proportion (%)
$T_1 + T_2$	219.26	54.1	128.87	31.8	37.61	9.3	11.90	2.9	5.46	1.4	1.88	0.5
$T_1 + T_2 + T_3$	222.96	55.1	129.96	32.1	35.68	8.8	10.34	2.6	4.43	1.1	1.63	0.4

Under the two construction scenarios of dry-farming wide terraces, micro and slight erosion were the main erosion types, collectively covering 86.0–87.1% of the research area, whereas moderate and strong erosion accounted for 11.4–12.2%, and very strong and severe erosion accounted for only 1.5–1.8%. Compared with the current soil erosion intensity, if the two scenarios can be implemented, the areas of micro and slight erosion will increase, while those of moderate to severe erosion will decrease (Table 6). In general, the sediment reduction potential was significant under the construction scenarios of dry-farming wide terraces.

4. Discussion

4.1. Distribution Patterns and Driving Factors of Soil Erosion

This study evaluated soil erosion intensity and analyzed its distribution pattern in the research area during 2016–2020. The total area of micro and slight erosion accounted for 82.2%, while the area of moderate to severe erosion accounted for 17.8%. Micro and slight erosion were primarily concentrated in the eastern and southern areas, whereas moderate to severe erosion was mainly distributed in the western and northern areas, as well as in river valleys and gullies. Ningxia and Gansu provinces exhibited the most severe soil erosion, whereas Henan Province demonstrated the lightest soil erosion. These findings were broadly consistent with previous studies [56,57] in two respects: micro and slight erosion were dominant in the Loess Plateau, and the main hotspots of moderate to severe erosion were concentrated in the western and northern parts of the region.

The distribution pattern of soil erosion intensity was the result of the action of multiple factors. Specifically, in the eastern and southern areas, although the *R* factor was high, the *C*, *P*, and *LS* factors were low; thus, soil erosion in these areas remained relatively weak. Conversely, in the western and northern areas, the combination of low *R* values and high *C*, *P*, and *LS* values led to severe soil erosion. The erosion distribution pattern indicated that soil erosion control should prioritize the western and northern areas of the study region. The significant geographic variability of the erosion pattern drivers further indicated the critical role of vegetation restoration and land surface modification in soil erosion control [56,58]. It should also be noted that these results are based on the

RUSLE framework, which mainly reflects sheet and rill erosion and may not fully capture gully-dominated processes on some sloping farmland.

4.2. Construction Suitability of Dry-Farming Wide Terraces and Key Influencing Factors

This study developed a suitability evaluation index system incorporating 12 influencing factors and evaluated the construction suitability of dry-farming wide terraces. Compared with previous studies that mainly emphasized topographic and soil-related conditions [59,60], this study expanded earlier approaches by incorporating a broader set of factors, including soil erosion intensity, water availability, and socioeconomic conditions, thus providing a more multidimensional basis for terrace planning in semi-arid and semi-humid regions.

The suitability evaluation revealed the areas, spatial distributions and environmental distinctions of the four construction suitability grades. The reliability of the suitability evaluation results was partly supported by comparing the spatial distribution between the predicted suitability zones and the existing terraces. The concentrated areas of the highly suitable, suitable, and barely suitable classes were broadly consistent with the existing terrace pattern, and the cumulative overlap ratio reached 37.8%. The incomplete coincidence is reasonable because the existing terraces reflect historical construction practices and include low-standard or narrow terraces, whereas this study evaluated the suitability of dry-farming wide terraces under current technical and planning conditions.

In terms of suitability grade and construction intensity, the top three provinces were Shanxi, Shaanxi, and Gansu, and the top three prefecture-level cities were Yulin, Yan'an, and Qingyang. A particularly notable contrast was observed in the Ningxia Hui Autonomous Region. Although Ningxia exhibited the most severe soil erosion in the study area, it had relatively limited areas suitable for wide terrace construction. This contrast suggests that severe erosion alone does not necessarily imply high construction suitability, because wide terrace construction is also constrained by other factors within the suitability framework, especially terrain conditions and implementation accessibility. Therefore, the Ningxia case further demonstrates the necessity of a multidimensional suitability framework rather than a single-factor judgment based only on erosion severity.

This study identified that slope, transportation convenience, and soil erosion intensity were the key influencing factors for the construction suitability of dry-farming wide terraces. The prominence of these factors reflects both their environmental and engineering importance in the Loess Plateau, and the weighting structure of the suitability model. Previous studies have shown that terraces, as an important soil and water conservation measure in the Loess Plateau, can substantially reduce soil loss in areas with slopes greater than 10° [61,62]. Therefore, slope became the most critical determinant of the construction suitability of dry-farming wide terraces on sloping farmland in the Loess Plateau. In this study, the 5–25° slope range was first selected according to the slope of sloping farmland and relevant policies [53,54] for terrace construction in the research area, and suitability classes were then further differentiated within this range through the combined effects of multiple factors. The identified highly suitable areas also exhibit moderate slopes (with an average slope of 11.49°) and other favorable natural and socioeconomic conditions. Transportation convenience influences the engineering difficulty and cost of terrace construction, as well as the accessibility of human agricultural activities [63]. Areas closer to roads generally have higher construction priority not only because of lower construction costs and management convenience, but also because they are more favorable for machinery access, material transport, and large-scale implementation of wide terrace construction. Additionally, the soil erosion modulus serves as an indicator of the severity of soil and water loss in farmland, and areas with higher erosion modulus stand to gain greater ecological and

economic benefits from terrace construction. The variations in the construction suitability of dry-farming wide terraces across provinces and cities were strongly influenced by these key factors.

Nevertheless, high construction suitability does not necessarily imply long-term sustainability. The long-term effectiveness of dry-farming wide terraces also depends on maintenance conditions, accessibility for farming activities, and their stability under rainfall and erosion stress. Therefore, future planning should extend beyond construction suitability and incorporate the long-term sustainability of terrace management and ecological benefits.

4.3. Discussion on the Sediment Reduction Potential of Dry-Farming Wide Terraces

This study integrated soil erosion intensity and terrace construction suitability to assess the sediment reduction potential of dry-farming wide terraces under two assumed implementation scenarios. Under the $T_1 + T_2$ and $T_1 + T_2 + T_3$ scenarios, the average soil erosion modulus is projected to decrease by 16.6% and 22.0%, respectively, while the area of moderate to severe erosion is projected to decrease by 3.7% and 4.9%, respectively. In practical terms, these scenario-based reductions suggest that wide terrace construction could shift part of the study area from higher-risk erosion classes to lower-risk classes, thereby contributing to regional soil and water conservation, reducing sediment-source pressure in erosion-prone sloping farmland, and improving the overall spatial pattern of erosion control.

These findings were broadly consistent with previous studies and provided additional support for the role of dry-farming terraces in sediment reduction and ecological improvement. A national meta-analysis of terracing practices in China reported average runoff and sediment reductions of 48.9% and 53.0%, respectively [64]. At the catchment scale in the Chinese Loess Plateau, Bai et al. [65] estimated an average sediment reduction rate of 24.52% during sediment routing. At the same time, the magnitude of reduction reported here is lower than some of the larger reductions cited in the literature, which is reasonable for several reasons. First, this study was conducted at a regional scale under partial implementation scenarios, rather than under complete terrace coverage or plot-scale experimental conditions. Second, this study specifically evaluated the sediment-reduction potential of dry-farming wide terraces, whereas some previous studies assessed the overall conservation effects of terraces without distinguishing terrace width or terrace type. Therefore, differences in the evaluation object may partly explain why the reduction magnitude reported here is lower than some values in the literature. In addition, the sediment-reduction effect of terraces is influenced by terrace width, plot area, slope gradient, rainfall regime, and spatial arrangement. Previous studies have also shown that terrace geometry and spatial arrangement are important determinants of conservation performance. Han et al. [66] identified terrace width as an important cross-sectional parameter affecting slope erosion and nutrient losses; Jia et al. [67] showed that terrace width, terrace slope, and vegetation restoration influenced soil and water conservation benefits under extreme precipitation; and Guan et al. [68] demonstrated that the water- and sediment-reduction effects of terraces are closely related not only to terrace scale, but also to their spatial configuration at the basin scale. Therefore, although the absolute values reported in different studies are not directly identical, the present results are broadly consistent with the available evidence and support the view that dry-farming wide terraces can provide substantial sediment-reduction benefits when reasonably designed and distributed in erosion-prone areas.

4.4. Limitations and Future Research

Despite providing a regional-scale evaluation of the construction suitability and sediment reduction potential of dry-farming wide terraces, this study still has several limitations.

First, although the datasets were obtained from authoritative sources and are widely used in regional environmental studies, their reliability is not uniform across all variables and spatial scales. Data such as DEM, land use, NDVI, and precipitation observations provide relatively strong support for regional analysis, whereas coarser or older datasets, including soil organic carbon, population density, transportation networks, and village/town-center data, are less capable of representing fine-scale spatial heterogeneity. Therefore, the present results are more reliable for regional pattern identification than for site-specific engineering application.

Second, spatial resolution and temporal inconsistency among datasets may affect the fine-scale accuracy of the suitability results. Although all raster datasets were harmonized to 12.5 m for spatial overlay analysis, this resampling did not improve the intrinsic resolution of originally coarser inputs. In addition, datasets from different years, including 2000, 2007, 2015, 2016–2020, and 2020, may not fully represent current local conditions. For example, older accessibility-related data may underestimate present transportation convenience, and the 2015 terrace distribution dataset may not fully reflect recent terrace development. These uncertainties are more likely to affect suitability boundaries and local suitability estimates than the overall regional pattern.

Third, some key variables were derived through generalized regional processing. For example, precipitation and rainfall erosivity surfaces were generated from 79 meteorological stations by spatial interpolation, and NDVI was represented by a multiyear mean for 2016–2020. These treatments are appropriate for regional-scale assessment, but they may smooth short-term or local variability and, thus, introduce some uncertainty into the derived R and C factors.

Fourth, engineering input costs and economic benefits were not explicitly included in the evaluation framework. As a result, the present suitability map mainly reflects environmental, engineering, and accessibility conditions, but does not fully capture the economic feasibility of terrace implementation. Future studies should incorporate cost–benefit considerations to improve the practical value of suitability zoning.

Fifth, the study is also subject to model-related limitations. The soil erosion assessment was based on the RUSLE framework, which mainly reflects sheet and rill erosion. This was considered appropriate because the study focuses on sloping farmland rather than on specific gully systems. However, in some local areas affected by gully processes, RUSLE may not fully represent all erosion forms. In addition, the suitability evaluation relied on AHP and fuzzy membership functions, which involve expert judgment and, therefore, contain a degree of subjectivity. No formal sensitivity analysis of weights or membership assignments was conducted.

Finally, external validation of the suitability results remains limited. Although the predicted suitable areas were compared with the existing terrace distribution, this comparison served mainly as a plausibility check rather than full external validation. Moreover, the existing terrace dataset reflects historical construction outcomes under different technical standards and may include narrow or low-standard terraces, which are not fully equivalent to the dry-farming wide terraces evaluated in this study.

Taken together, these limitations do not negate the regional significance of this study, but indicate that the results are more suitable for regional planning and screening than for direct application to detailed engineering design and implementation.

5. Conclusions

This study conducted a comprehensive evaluation of the construction suitability and sediment reduction potential of dry-farming wide terraces on sloping farmland in the Loess Plateau. The areas classified as highly suitable, suitable, and barely suitable were

30,578.19 km^2, 29,311.69 km^2, and 17,300.60 km^2, respectively. Slope, transportation convenience, and soil erosion intensity were the key influencing factors for the construction suitability of dry-farming wide terraces. This indicates that regional terrace planning should give priority not only to erosion-prone areas, but also to locations with favorable terrain and implementation accessibility. In terms of suitability grade and construction intensity, the top three provinces were Shanxi, Shaanxi, and Gansu, and the top three prefecture-level cities were Yulin, Yan'an, and Qingyang. Although the Ningxia Hui Autonomous Region exhibited the most severe soil erosion, its area suitable for wide terrace construction was relatively limited because of constraints such as terrain conditions and implementation accessibility. This contrast further highlights the need for a multidimensional planning framework.

If two assumed construction schemes of wide terraces (one involving highly suitable and suitable areas, and the other involving highly suitable, suitable and barely suitable areas) can be implemented, the sloping farmland will be reclaimed by 59.89×10^3 km^2 and 77.19×10^3 km^2, respectively. Under these assumed scenarios, the average soil erosion modulus is projected to decrease by up to 22.0%, indicating considerable sediment reduction potential of dry-farming wide terraces on sloping farmland in the Loess Plateau. These findings emphasize the importance of strategic terrace planning for ecological improvement and soil erosion control.

The main contribution of this study lies in the integration of construction suitability assessment and sediment reduction potential evaluation for dry-farming wide terraces at the regional scale of the Loess Plateau. Unlike previous studies that mainly focused either on terrace erosion-control effects or on land suitability alone, this study developed a comprehensive and operational evaluation framework by combining the RUSLE model, the AHP method, fuzzy membership functions, and a comprehensive index model. This framework not only identified the key influencing factors and spatially suitable areas for wide terrace construction, but also quantified the potential erosion-control benefits of wide terrace implementation under different assumed construction schemes.

Overall, this study provides a comprehensive, multidimensional decision-making framework for wide terrace planning in semi-arid and semi-humid regions, and confirms the substantial potential of dry-farming wide terraces in controlling soil erosion in the Loess Plateau. Future research should further improve the evaluation by incorporating higher-resolution spatial data, engineering input costs, and the long-term socioeconomic benefits of wide terrace construction.

Author Contributions: Conceptualization, J.F. and Y.H.; methodology, J.F. and Y.H.; software, Y.H., W.W. and R.D.; validation, Y.H., W.W. and J.F.; formal analysis, Y.H. and B.L.; investigation, W.W. and R.D.; resources, J.F.; data curation, X.C.; writing—original draft preparation, Y.H. and J.F.; writing—review and editing, Y.H. and J.F.; visualization, W.W. and R.D.; supervision, J.F.; project administration, J.F.; funding acquisition, J.F. All authors have read and agreed to the published version of the manuscript.

Funding: This research was funded by the National Key Research and Development Program of China (2022YFF1300805) and the National Natural Science Foundation of China (U2243210).

Data Availability Statement: No new data were created or analyzed in this study. Data sharing is not applicable to this article.

Conflicts of Interest: The authors declare no conflict of interest.

References

1. Li, Z.B.; Zhu, B.B.; Li, P. Advancement in study on soil erosion and soil and water conservation. *Acta Pedol. Sin.* **2008**, *45*, 802–809. (In Chinese)
2. Dang, T.; Mu, X.; Sun, W.; Gao, P.; Zhao, G. Review of quickly discriminating approaches of terrace information based on high-resolution remote sensing images. *Yellow River* **2017**, *39*, 85–89. (In Chinese)
3. Lü, H.; Zhu, Y.; Skaggs, T.H.; Yu, Z. Comparison of measured and simulated water storage in dryland terraces of the Loess Plateau, China. *Agric. Water Manag.* **2009**, *96*, 299–306. [CrossRef]
4. Sun, W.; Shao, Q.; Liu, J.; Zhai, J. Assessing the effects of land use and topography on soil erosion on the Loess Plateau in China. *Catena* **2014**, *121*, 151–163. [CrossRef]
5. Posthumus, H.; Stroosnijder, L. To terrace or not: The short-term impact of bench terraces on soil properties and crop response in the Peruvian Andes. *Environ. Dev. Sustain.* **2010**, *12*, 263–276. [CrossRef]
6. Wei, W.; Chen, D.; Wang, L.; Daryanto, S.; Chen, L.; Yu, Y.; Lu, Y.; Sun, G.; Feng, T. Global synthesis of the classifications, distributions, benefits and issues of terracing. *Earth-Sci. Rev.* **2016**, *159*, 388–403. [CrossRef]
7. Yang, L.; Feng, Q.; Chen, L. Ecosystem services of soil and water conservation measures on the Loess Plateau. *Resour. Sci.* **2020**, *42*, 87–95. (In Chinese) [CrossRef]
8. Dang, W.; Dang, T.; Zhang, Q. Suggestions on vigorously constructing dry-farming terraces and innovating management mechanisms in the Loess Plateau. *China Water Resour.* **2020**, *12*, 55–57. (In Chinese)
9. Dang, W. Recommendations and reflections on strengthening grassroots soil and water conservation research on the Loess Plateau. *China Water Resour.* **2019**, *21*, 6–8. (In Chinese)
10. Ahmed, G.B.; Shariff, A.R.M.; Balasundram, S.K.; Abdullah, A.F.B. Agricultural land suitability analysis evaluation based multi criteria and GIS approach. *IOP Conf. Ser. Earth Environ. Sci.* **2016**, *37*, 012044. [CrossRef]
11. Kalogirou, S. Expert systems and GIS: An application of land suitability evaluation. *Comput. Environ. Urban Syst.* **2002**, *26*, 89–112. [CrossRef]
12. Kılıç, M.; Gündoğan, R.; Günal, H. An illustration of a sustainable agricultural land suitability assessment system with a land degradation sensitivity. *Environ. Dev. Sustain.* **2024**, *26*, 6085–6107. [CrossRef]
13. Akıncı, H.; Özalp, A.Y.; Turgut, B. Agricultural land use suitability analysis using GIS and AHP technique. *Comput. Electron. Agric.* **2013**, *97*, 71–82. [CrossRef]
14. Bagheri, M.; Ibrahim, Z.; Mansor, S.; Manaf, L.A.; Akhir, M.F.; Talaat, W.I.A.W.; Beiranvand Pour, A. Land-use suitability assessment using Delphi and analytical hierarchy process (D-AHP) hybrid model for coastal city management: Kuala Terengganu, Peninsular Malaysia. *ISPRS Int. J. Geo-Inf.* **2021**, *10*, 621. [CrossRef]
15. Binte Mostafiz, R.; Noguchi, R.; Ahamed, T. Agricultural land suitability assessment using satellite remote sensing-derived soil-vegetation indices. *Land* **2021**, *10*, 223. [CrossRef]
16. Cao, X.; Wei, C.; Xie, D. Evaluation of scale management suitability based on the entropy-TOPSIS method. *Land* **2021**, *10*, 416. [CrossRef]
17. Kılıç, O.M.; Ersayın, K.; Günal, H.; Khalofah, A.; Alsubeie, M.S. Combination of fuzzy-AHP and GIS techniques in land suitability assessment for wheat (*Triticum aestivum*) cultivation. *Saudi J. Biol. Sci.* **2022**, *29*, 2634–2644. [CrossRef]
18. Mendas, A.; Mebrek, A.; Mekranfar, Z. Comparison between two multicriteria methods for assessing land suitability for agriculture: Application in the area of Mleta in western part of Algeria. *Environ. Dev. Sustain.* **2021**, *23*, 9076–9089. [CrossRef]
19. Chen, Y.; Yu, J.; Khan, S. Spatial sensitivity analysis of multi-criteria weights in GIS-based land suitability evaluation. *Environ. Model. Softw.* **2010**, *25*, 1582–1591. [CrossRef]
20. Tiwari, A.; Ajmera, S. Land suitability assessment for agriculture using analytical hierarchy process and weighted overlay analysis in ArcGIS ModelBuilder. In *Recent Trends in Civil Engineering: Select Proceedings of ICRTICE 2019*; Springer: Singapore, 2021; pp. 735–762.
21. Feng, J.; Wei, W.; Pan, D. Effects of rainfall and terracing-vegetation combinations on water erosion in a loess hilly area, China. *J. Environ. Manag.* **2020**, *261*, 110247. [CrossRef]
22. Ran, Q.; Chen, X.; Hong, Y.; Ye, S.; Gao, J. Impacts of terracing on hydrological processes: A case study from the Loess Plateau of China. *J. Hydrol.* **2020**, *588*, 125045. [CrossRef]
23. Shi, S.; Jiang, D. Impacts of several soil and water conservation measures on strengthening rainfall infiltration and reducing sediment yield. *Res. Soil Water Conserv.* **1994**, *1*, 82–88. (In Chinese)
24. Liu, X.; Wang, F.; Yang, S.; Li, X.; Ma, H.; He, X. Sediment reduction effect of level terrace in the hilly–gully region of the Loess Plateau. *J. Hydraul. Eng.* **2014**, *45*, 793–800. (In Chinese)
25. Ma, H.; Li, J.; He, X.; Liu, X.; Wang, F. Status and sediment reduction effects of level terrace in the Loess Plateau. *Yellow River* **2015**, *37*, 89–93. (In Chinese)
26. Gao, Y.; Liu, X.; Han, X. Impacts of terrace application on sediment-yield patterns and thresholds in a Loess Plateau watershed. *J. Basic Sci. Eng.* **2020**, *28*, 535–545. (In Chinese)

27. Hussein, M.H.; Amien, I.M.; Kariem, T.H. Designing terraces for the rainfed farming region in Iraq using the RUSLE and hydraulic principles. *Int. Soil Water Conserv. Res.* **2016**, *4*, 39–44. [CrossRef]
28. Rončević, V.; Zlatić, M.; Todosijević, M. Environmental and economic effects of investments in sustainable land management in the basin of Sutilovac stream. *Glas. Šum. Fak.* **2019**, *119*, 213–232. [CrossRef]
29. Tričković, N.; Rončević, V.; Živanović, N.; Grujić, T.; Stefanović, L.; Jovanović, N.; Zlatić, M. Ecological and economic effects of applying the future agricultural production structure model (FAPSMS): The case study of the Barička River Basin. *Sustainability* **2023**, *15*, 8434. [CrossRef]
30. Benavidez, R.; Jackson, B.; Maxwell, D.; Norton, K. A review of the (Revised) Universal Soil Loss Equation ((R)USLE): With a view to increasing its global applicability and improving soil loss estimates. *Hydrol. Earth Syst. Sci.* **2018**, *22*, 6059–6086. [CrossRef]
31. Tang, Q.; Xu, Y.; Bennett, S.J.; Li, Y. Assessment of soil erosion using RUSLE and GIS: A case study of the Yangou watershed in the Loess Plateau, China. *Environ. Earth Sci.* **2015**, *73*, 1715–1724. [CrossRef]
32. Renard, K.G.; Foster, G.R.; Weesies, G.A.; McCool, D.K.; Yoder, D.C. *Predicting Soil Erosion by Water: A Guide to Conservation Planning with the Revised Universal Soil Loss Equation (RUSLE)*; U.S. Department of Agriculture: Washington, DC, USA, 1997; Agriculture Handbook No. 703.
33. Tian, P.; Zhu, Z.; Yue, Q.; He, Y.; Zhang, Z.; Hao, F.; Guo, W.; Chen, L.; Liu, M. Soil erosion assessment by RUSLE with improved P factor and its validation: Case study on mountainous and hilly areas of Hubei Province, China. *Int. Soil Water Conserv. Res.* **2021**, *9*, 433–444. [CrossRef]
34. Tian, P.; Tian, X.; Geng, R.; Zhao, G.; Yang, L.; Mu, X.; Gao, P.; Sun, W.; Liu, Y. Response of soil erosion to vegetation restoration and terracing on the Loess Plateau. *Catena* **2023**, *227*, 107103. [CrossRef]
35. Wang, C.; Wang, X.; Fu, X.; Zhang, X.; Wang, Y. Dynamic changes and sediment reduction effect of terraces on the Loess Plateau. *Remote Sens.* **2025**, *17*, 4021. [CrossRef]
36. Yan, R.; Zhang, X.; Yan, S.; Chen, H. Estimating soil erosion response to land use/cover change in a catchment of the Loess Plateau, China. *Int. Soil Water Conserv. Res.* **2018**, *6*, 13–22. [CrossRef]
37. Jiang, C.; Wang, F.; Zhang, H.; Dong, X. Quantifying changes in multiple ecosystem services during 2000–2012 on the Loess Plateau, China, as a result of climate variability and ecological restoration. *Ecol. Eng.* **2016**, *97*, 258–271. [CrossRef]
38. Fu, B. Soil erosion and its control in the Loess Plateau of China. *Soil Use Manag.* **1989**, *5*, 76–82. [CrossRef]
39. Du, Y.; Zhao, J.; Huang, Q. Quantitative driving analysis of climate on potential evapotranspiration in Loess Plateau incorporating synergistic effects. *Ecol. Indic.* **2022**, *141*, 109076. [CrossRef]
40. Shangguan, W.; Dai, Y.; Duan, Q.; Liu, B.; Yuan, H. A global soil data set for earth system modeling. *J. Adv. Model. Earth Syst.* **2014**, *6*, 249–263. [CrossRef]
41. Cao, R.; Xu, Z.; Chen, Y.; Chen, J.; Shen, M. Reconstructing high-spatiotemporal-resolution (30 m and 8-days) NDVI time-series data for the Qinghai–Tibetan Plateau from 2000–2020. *Remote Sens.* **2022**, *14*, 3648. [CrossRef]
42. Dong, S.; Xin, L.; Li, S.; Xie, H.; Zhao, Y.; Wang, X.; Li, X.; Song, H.; Lu, Y. Extent and spatial distribution of terrace abandonment in China. *J. Geogr. Sci.* **2023**, *33*, 1361–1376. [CrossRef]
43. Zhu, G.; Shangguan, Z.; Hu, X.; Deng, L. Effects of land use changes on soil organic carbon, nitrogen and their losses in a typical watershed of the Loess Plateau, China. *Ecol. Indic.* **2021**, *133*, 108443. [CrossRef]
44. Lebakula, V.; Sims, K.; Reith, A.; Rose, A.; McKee, J.; Coleman, P.; Kaufman, J.; Urban, M.; Jochem, C.; Whitlock, C.; et al. LandScan global 30 arcsecond annual global gridded population datasets from 2000 to 2022. *Sci. Data* **2025**, *12*, 495. [CrossRef] [PubMed]
45. Zhang, W.; Xie, Y.; Liu, B. A method for estimating rainfall erosivity using daily rainfall amounts. *Geogr. Sci.* **2002**, *22*, 705–711. (In Chinese)
46. Williams, J.R.; Dyke, P.T.; Jones, C.A. EPIC: A model for assessing the effects of erosion on soil productivity. In *Developments in Environmental Modelling*; Elsevier: Amsterdam, The Netherlands, 1983; pp. 553–572.
47. Liu, B.Y.; Nearing, M.A.; Shi, P.J.; Jia, Z.W. Slope length effects on soil loss for steep slopes. *Soil Sci. Soc. Am. J.* **2000**, *64*, 1759–1763. [CrossRef]
48. Van der Knijff, J.M.F.; Jones, R.J.A.; Montanarella, L. *Soil Erosion Risk Assessment in Italy (EUR 19022 EN)*; European Soil Bureau, Joint Research Centre, European Commission: Ispra, Italy, 2002.
49. Gao, G.Y.; Fu, B.J.; Lü, Y.H.; Liu, Y.; Wang, S.; Zhou, J. Coupling the modified SCS–CN and RUSLE models to simulate hydrological effects of restoring vegetation in the Loess Plateau of China. *Hydrol. Earth Syst. Sci.* **2012**, *16*, 2347–2364. [CrossRef]
50. Tanyaş, H.; Kolat, Ç.; Süzen, M.L. A new approach to estimate cover-management factor of RUSLE and validation of RUSLE model in the watershed of Kartalkaya Dam. *J. Hydrol.* **2015**, *528*, 584–598. [CrossRef]
51. Saaty, T.L. Time dependent decision-making; dynamic priorities in the AHP/ANP: Generalizing from points to functions and from real to complex variables. *Math. Comput. Model.* **2007**, *46*, 860–891. [CrossRef]
52. Tashayo, B.; Honarbakhsh, A.; Azma, A.; Akbari, M. Combined fuzzy AHP–GIS for agricultural land suitability modeling for a watershed in southern Iran. *Environ. Manag.* **2020**, *66*, 364–376. [CrossRef]

53. Xu, Y.; Yang, B.; Tang, Q.; Liu, G.; Liu, P. Analysis of comprehensive benefits of transforming slope farmland to terraces on the Loess Plateau: A case study of the Yangou Watershed in Northern Shaanxi Province, China. *J. Mt. Sci.* **2011**, *8*, 448–457. [CrossRef]
54. Liu, N. *Water and Soil Conservation Law of the People's Republic of China*; Standing Committee of the National People's Congress: Beijing, China, 2010. (In Chinese)
55. Jin, G.; Wang, Z.; Hu, X.; Hu, S.; Zhang, D. Land suitability evaluation on the Qinghai–Tibet Plateau based on a fuzzy evidence–weight model. *Trans. Chin. Soc. Agric. Eng.* **2013**, *29*, 214–250. (In Chinese)
56. Liu, P.; Guo, B.; Zhang, R.; Wang, L. Spatial–temporal evolution pattern of soil erosion and its dominant factors on the Loess Plateau from 2000 to 2020. *Land* **2024**, *13*, 1944. [CrossRef]
57. Tao, W.; Liu, S.; Wang, Q.; Su, L.; Sun, Y. Spatiotemporal characteristics of soil erosion on the Chinese Loess Plateau and strategies for vegetation management. *J. Soil Sci. Plant Nutr.* **2024**, *24*, 4439–4456. [CrossRef]
58. Yao, Z.; Huang, Y.; Zhang, Y.; Yang, Q.; Yang, M. Analysis of the spatial–temporal characteristics of vegetation cover changes in the Loess Plateau from 1982 to 2022. *Land* **2025**, *14*, 303. [CrossRef]
59. Stanchi, S.; Freppaz, M.; Agnelli, A.; Reinsch, T.; Zanini, E. Properties, best management practices and conservation of terraced soils in southern Europe (from Mediterranean areas to the Alps): A review. *Quat. Int.* **2012**, *265*, 90–100. [CrossRef]
60. Tarolli, P.; Preti, F.; Romano, N. Terraced landscapes: From an old best practice to a potential hazard for soil degradation due to land abandonment. *Anthropocene* **2014**, *6*, 10–25. [CrossRef]
61. Liu, X.; He, B.; Li, Z.; Zhang, J.; Wang, L.; Wang, Z. Influence of land terracing on agricultural and ecological environment in the Loess Plateau regions of China. *Environ. Earth Sci.* **2011**, *62*, 797–807. [CrossRef]
62. Gao, H.; Li, Z.; Li, P.; Jia, L.; Zhang, X. Quantitative analysis of the effects of terrace construction and check-dam siltation on soil erosion. *Acta Geogr. Sin.* **2012**, *67*, 599–608. (In Chinese)
63. Li, L.; Zhu, G.; Wu, D.; Xu, H.; Ma, P.; Liu, J.; Li, Z.; He, Y.; Li, C.; Wu, P. Land suitability assessment for supporting transport planning based on carrying capacity and construction demand. *PLoS ONE* **2021**, *16*, e0246374. [CrossRef] [PubMed]
64. Chen, D.; Wei, W.; Chen, L. Effects of terracing practices on water erosion control in China: A meta-analysis. *Earth-Sci. Rev.* **2017**, *173*, 109–121. [CrossRef]
65. Bai, J.; Yang, S.; Zhang, Y.; Liu, X.; Guan, Y. Assessing the impact of terraces and vegetation on runoff and sediment routing using the time-area method in the Chinese Loess Plateau. *Water* **2019**, *11*, 803. [CrossRef]
66. Han, Y.; Yang, P.; Wang, Y. Effect of level terraces of different widths on slope erosion and nutrient losses under rainfall condition. *Fresenius Environ. Bull.* **2015**, *24*, 3274–3280.
67. Jia, H.; Wang, X.; Sun, W.; Mu, X.; Gao, P.; Zhao, G.; Li, Z. Estimation of soil erosion and evaluation of soil and water conservation benefit in terraces under extreme precipitation. *Water* **2022**, *14*, 1675. [CrossRef]
68. Guan, Y.; Yang, S.; Wang, J.; Bai, J.; Liu, X.; Zhao, C.; Lou, H.; Chen, K. Effects of varying the spatial configuration and scale of terraces on water and sediment loss based on scenario simulation within the Chinese Loess Plateau. *Sci. Total Environ.* **2023**, *869*, 162522. [CrossRef]

Disclaimer/Publisher's Note: The statements, opinions and data contained in all publications are solely those of the individual author(s) and contributor(s) and not of MDPI and/or the editor(s). MDPI and/or the editor(s) disclaim responsibility for any injury to people or property resulting from any ideas, methods, instructions or products referred to in the content.